

Structure and Visible-Light Photocatalytic Performance of Zinc Cyanamide Composite Photocatalysts (Postprint)

Authors: Rong Fengming, Wang Yu, Zhang Xia

Date: 2017-11-21T00:00:00+00:00

Abstract

Zinc cyanamide (ZnNCN) particles were prepared via ligand exchange reaction between zinc salt, ammonia solution, and aqueous cyanamide solution. Silver cyanamide (Ag₂NCN)/ZnNCN composite particles were subsequently fabricated by blending silver salt in the precursor salt solution and employing the same ligand exchange reaction process. The structure of the photocatalysts was characterized using X-ray diffraction (XRD), scanning electron microscopy (SEM), Fourier transform infrared spectroscopy (FT-IR), and ultraviolet-visible (UV-Vis) absorption spectroscopy. The results demonstrated that pristine ZnNCN exhibited petal-like particle morphology and was a wide-bandgap semiconductor material ($E_g=4.66$ eV). The morphology of Ag₂NCN/ZnNCN composite particles differed substantially from both pristine ZnNCN and Ag₂NCN, with the two metal cyanamides combining via weak physical interactions to form a heterostructure. The spectral response range of the composite particles extended into the visible light region, with a bandgap $E_g=2.05$ eV. The photocatalytic activity of ZnNCN and Ag₂NCN/ZnNCN composite particles under xenon lamp irradiation was investigated using rhodamine B as the target pollutant for photocatalytic degradation. Compared with pristine ZnNCN and a mechanical mixture of Ag₂NCN and ZnNCN, the Ag₂NCN/ZnNCN composite particles exhibited enhanced photocatalytic performance, following first-order reaction kinetics.

Full Text

Structure and Visible-Light Induced Photocatalytic Activity of Zinc Cyanamide Based Photocatalysts

RONG Fengming, WANG Yu, ZHANG Xia

Department of Chemistry, College of Sciences, Northeastern University,

Shenyang 110819, China

Correspondent: ZHANG Xia, professor, Tel: (024)83683429, Email: xzhang@mail.neu.edu.cn

Supported by National Natural Science Foundation of China (No. 21501023) and National Undergraduate Innovation and Entrepreneurship Training Program (No. 201610145019)

Manuscript received 2017-04-11, **in revised form** 2017-05-09

Abstract

Semiconductor-based photocatalytic technology, using abundant and renewable sunlight as an induced light source, represents an emerging successful approach to address global energy and environmental challenges. Considerable efforts have been devoted to developing novel photocatalysts with good sunlight response and high quantum conversion efficiency. In this work, single ZnNCN microparticles were prepared by ligand exchange reaction between zinc salt, ammonia, and cyanamide. Additionally, Ag NCN/ZnNCN heterostructures were fabricated using the same ligand exchange process but with silver salt mixed together with zinc salt. The samples were characterized by XRD, SEM, infrared spectroscopy (FT-IR), and ultraviolet-visible spectrometry (UV-Vis). The results showed that single ZnNCN formed flower-like particles with a wide band gap ($E_g = 4.66$ eV). Compared with single ZnNCN, the Ag NCN/ZnNCN composite particles exhibited different morphology with rough surfaces, and physical interaction existed between the two kinds of metal cyanamides in the composites. Due to the heterostructure formation, the light response spectrum of Ag NCN/ZnNCN composite particles extended to the visible light region, and the band gap narrowed to 2.05 eV. The photocatalytic activity of Ag NCN/ZnNCN composite particles in degrading Rhodamine B under xenon irradiation was investigated, with single ZnNCN and a mechanical mixture of Ag NCN and ZnNCN tested under the same conditions for comparison. The Ag NCN/ZnNCN heterostructure showed apparently enhanced photocatalytic activity, following first-order reaction kinetics.

KEY WORDS visible-light photocatalysis, zinc cyanamide, silver cyanamide, ligand exchange reaction

Introduction

With the development of social economy, environmental pollution and energy shortage have become major challenges facing humanity. The discovery of photocatalysis as an environmentally friendly technology provides new solutions to these problems. In 1972, Fujishima and Honda [1] first reported that TiO semiconductor electrodes could split water under illumination. Subsequently, Carey et al. [2] demonstrated that TiO-water systems could degrade various refractory organic compounds under UV irradiation. Since then, photocatalytic

reactions of wide-bandgap semiconductor materials represented by TiO₂ have been extensively studied. However, because wide-bandgap semiconductors can only be excited by UV light, their utilization of solar energy is low, limiting their practical applications. Developing novel, efficient visible-light-responsive photocatalytic materials is currently a hot research topic in photocatalysis [3-5].

The cyanamide ion ([NCN]²⁻) is a linear triatomic ion that can form metal-metal bridging compounds with various metals [6-10]. In the [NCN]²⁻ structure, the C and N atoms undergo sp² hybridization to form a delocalized conjugated system, and the electron delocalization characteristics of its HOMO and LUMO orbitals are more similar to the electronic structure features of carbides or sulfides [11,12]. The [NCN]²⁻ ion has two different electronic structural states: the symmetric structure [N=C=N]²⁻ [11-17] and the asymmetric structure [N-C-N]²⁻ [18-21]. These two structures are analogous to the resonance structures of benzene rings. During the photoresponse process, photogenerated electrons can achieve efficient charge migration through conversion between the two resonance structures [22], reducing electron-hole recombination and improving the quantum conversion efficiency of photocatalysts. Therefore, the structural characteristics determine that metal cyanamide complexes may have good visible-light response and photocatalytic performance. In 2013, Zhao et al. [22] first reported the photocatalytic degradation activity of organic dyes by nano- and micro-sized Ag NCN particles. In 2015, our research group [23,24] synthesized TiO₂-Ag NCN composite particles and found they had good photocatalytic hydrogen production ability due to their unique band structure.

Currently, reports on metal cyanamides mostly focus on crystal structure synthesis, while studies on their photocatalytic performance are relatively scarce. In this work, ZnNCN ([Zn-N-C N]) was synthesized by a simple ligand exchange method, and its band structure and photocatalytic activity were investigated. To extend the spectral absorption range of ZnNCN to the visible region, Ag NCN/ZnNCN composite particles were synthesized, and their structure and enhanced visible-light photocatalytic activity were studied.

1. Experimental

1.1 Preparation of Photocatalysts

The experimental materials included AgNO₃ (purity > 99.8%), Zn(NO₃)₂ (purity > 99%), ammonia solution (mass fraction 25%), and aqueous cyanamide solution (mass fraction 50%), all of which were analytically pure and used without further treatment. Deionized water was used throughout the experiments.

The synthesis procedure for ZnNCN was as follows: 1.78 g of Zn(NO₃)₂ · 6H₂O was dissolved in 60 mL deionized water; 40 mL of 3 mol/L NH₃ · H₂O was added dropwise to obtain a transparent solution; then 80 mL of 0.9 wt% aqueous cyanamide solution was added dropwise with stirring for 30 min to obtain white ZnNCN particles, which were centrifuged, washed, and vacuum-dried at 60 °C.

The synthesis procedure for Ag NCN was: 0.51 g AgNO₃ was dissolved in 30 mL deionized water; 60 mL of 3 mol/L NH₃ · H₂O was added dropwise to obtain a transparent solution with continued stirring for 20 min; then 30 mL of 0.9 wt% aqueous cyanamide solution was added dropwise with stirring for 30 min to obtain a dark yellow solid, which was centrifuged, washed, and vacuum-dried at 60 °C.

The synthesis procedure for Ag NCN/ZnNCN composite photocatalyst was: 0.51 g AgNO₃ was dissolved in 30 mL deionized water; separately, 1.78 g Zn(NO₃)₂ · 6H₂O was dissolved in 60 mL deionized water; the two solutions were mixed thoroughly. Then 60 mL of 3 mol/L NH₃ · H₂O was added dropwise to obtain a transparent solution with stirring for 20 min; subsequently, 30 mL of 0.9 wt% aqueous cyanamide solution was added dropwise with stirring for 30 min to obtain a dark yellow solid, which was centrifuged, washed, and vacuum-dried at 60 °C to yield the dark yellow Ag NCN/ZnNCN composite photocatalyst.

1.2 Structural Characterization

Crystal structures were determined by X-ray diffraction (XRD) using a D/max-2500PC diffractometer (Cu K_α, tube voltage 50 kV, tube current 100 mA, wavelength 0.15406 nm, graphite monochromator) with a scanning step of 0.02° and scanning range of 5°-90°. Morphology was observed using an EVO18 field-emission scanning electron microscope (SEM). Fourier transform infrared (FT-IR) spectra were recorded on a VERTEX-70 spectrometer using KBr pellets. UV-Vis diffuse reflectance spectra were measured on a Lambda-35 UV-Vis spectrophotometer in the wavelength range of 200-800 nm.

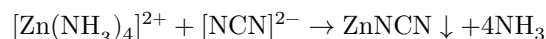
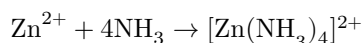
1.3 Photocatalytic Degradation Experiments

Photocatalytic degradation was performed using 80 mL of 1 × 10⁻⁵ mol/L Rhodamine B solution as the target pollutant, with 80 mg photocatalyst added and dispersed by ultrasonication. Before illumination, the suspension was magnetically stirred in the dark for 30 min to achieve adsorption equilibrium. A PLS-SXE300/300UV xenon lamp (300 W) was used as the light source for vertical irradiation of the reaction solution. Every 5 min, 4 mL of suspension was sampled, centrifuged at high speed, and the supernatant was analyzed using a TU-1900 UV-Vis spectrophotometer to measure the absorbance of Rhodamine B at its maximum absorption wavelength of 566 nm. The concentration change of Rhodamine B was determined from a calibration curve.

2. Results and Discussion

2.1 Structure of ZnNCN and Ag NCN/ZnNCN Composite Particles

In this work, ZnNCN particles were prepared through ligand exchange reaction between cyanamide ions ([NCN]²⁻) and NH₃ molecules. The reaction equations are as follows:



The SEM image of white ZnNCN particles is shown in [Figure 1: see original paper]a. The prepared ZnNCN exhibited a flaky morphology, with ZnNCN flakes stacking to form beautiful flower-like structures. Each flower-like ZnNCN cluster had a particle size smaller than 2 μm . [Figure 1: see original paper]b shows the SEM image of single Ag NCN particles, which exhibited a rectangular prism shape. The SEM image of Ag NCN/ZnNCN composite particles prepared from mixed Ag⁺ and Zn²⁺ solutions is shown in [Figure 1: see original paper]c. Compared with single ZnNCN particles ([Figure 1: see original paper]a), the composite particles showed significantly different morphology, with the flower-like structure disappearing and the particles becoming irregular in shape with rough surfaces. EDS analysis ([Figure 1: see original paper]d) indicated that the composite particles contained Zn and Ag with an atomic ratio of approximately 1:2. Comparing [Figure 1: see original paper]a, b, and c, the morphology of the composite metal cyanamide obtained under coexisting metal ion conditions differed from both single ZnNCN and Ag NCN, suggesting that the two metal cyanamides doped to form a heterostructure.

[Figure 2: see original paper]a shows the XRD patterns of ZnNCN, Ag NCN, and Ag NCN/ZnNCN composite particles. The XRD pattern of ZnNCN was basically consistent with its standard XRD data (PDF01-0788), with the only difference being two peaks of equal intensity at $2\theta = 28.05^\circ$ and 28.69° . The peak at 28.69° corresponds to ZnNCN diffraction, while the peak at 28.05° belongs to zinc carbodiimide ([Zn-N=C=N]) [25]. According to literature [25], [Zn-N-C N] and [Zn-N=C=N] are isomers with the same chemical composition and similar crystal structures, but different N-C bond lengths in the carbodiimide ([N=C=N]²⁻) and cyanamide ([N C-N]²⁻) ions lead to slightly different lattice parameters, resulting in coexistence of both crystal structures in ZnNCN solids. In the XRD pattern of Ag NCN/ZnNCN composite particles, characteristic diffraction peaks of both ZnNCN and Ag NCN (PDF70-523) were observed, confirming that the composite particles consisted of both ZnNCN and Ag NCN crystal structures.

[Figure 2: see original paper]b presents the FT-IR spectra of ZnNCN, Ag NCN, and Ag NCN/ZnNCN composite particles. The three samples showed similar absorption peak positions. Taking ZnNCN as an example, the absorption peak at 2043 cm^{-1} arises from the asymmetric stretching vibration of [NCN]²⁻, the peak at 1242 cm^{-1} corresponds to symmetric stretching vibration, and the peak at 677 cm^{-1} is due to deformation vibration of [NCN]²⁻ [24]. Additionally, the peak at 3421 cm^{-1} is the -OH stretching vibration, and 1629 cm^{-1} is the bending vibration of water molecules adsorbed on the ZnNCN surface, indicating that the synthesized ZnNCN particles contained some surface -OH groups. Compared

with single ZnNCN and Ag NCN particles, the asymmetric stretching vibration peak of $[\text{NCN}]^2$ in the Ag NCN/ZnNCN composite particles shifted from 2043 cm^{-1} to 1971 cm^{-1} . Moreover, no new characteristic absorption peaks appeared in the composite, indicating that ZnNCN and Ag NCN were not connected by specific covalent bonds but rather formed composite particles through weak physical interactions.

The UV-Vis diffuse reflectance absorption spectra of ZnNCN, Ag NCN, and Ag NCN/ZnNCN composite particles are shown in [Figure 3: see original paper]a. ZnNCN exhibited an absorption edge below 250 nm, indicating strong UV absorption capability. Compared with single ZnNCN, single Ag NCN showed significantly enhanced absorption in the visible region. The Ag NCN/ZnNCN composite particles displayed strong absorption peaks in both visible and UV regions, demonstrating excellent UV and visible light response activity.

For direct transition semiconductors, the absorbance at the absorption edge follows Equation (3) [26]:

$$A = C \frac{(h\nu - E_g)^{1/2}}{h\nu}$$

where C is a proportionality constant, A is absorbance, h is Planck's constant, ν is the frequency of incident photons, and E_g is the band gap energy. Mathematical transformation of Equation (3) yields Equation (4):

$$(A \times h\nu)^2 = C(h\nu - E_g)$$

Setting $C = 1$ and plotting $(A \times h\nu)^2$ versus $h\nu$, the band gap energy E_g can be obtained by extrapolating the linear portion of the curve to $(A \times h\nu)^2 = 0$. Based on the absorbance A and corresponding wavelength values from the UV-Vis diffuse reflectance spectra in [Figure 3: see original paper]a, the $(A \times h\nu)^2$ versus $h\nu$ curves for flower-like ZnNCN particles and Ag NCN/ZnNCN composite particles were obtained, as shown in [Figure 3: see original paper]b and c, respectively. The band gap energy of ZnNCN was determined to be $E_g = 4.71 \text{ eV}$, while that of Ag NCN/ZnNCN composite particles was $E_g = 2.05 \text{ eV}$, which is smaller than that of single Ag NCN (2.42 eV) [24].

2.2 Photocatalytic Performance of Ag NCN/ZnNCN Composite Photocatalyst

[Figure 4: see original paper] shows the photocatalytic degradation kinetics of Rhodamine B by Ag NCN/ZnNCN composite particles, single ZnNCN particles, and a mechanical mixture of ZnNCN and Ag NCN with the same composition as the composite. All three photocatalysts exhibited weak surface adsorption activity for Rhodamine B. Upon illumination, the concentration of Rhodamine

B solution decreased significantly in the presence of photocatalysts. The photocatalytic degradation activity followed the order: Ag NCN/ZnNCN composite particles > Ag NCN+ZnNCN mechanical mixture > single ZnNCN particles. The Ag NCN/ZnNCN composite particles showed the highest photocatalytic activity, achieving 95.2% degradation efficiency for Rhodamine B within 30 min. According to Zhao et al. [22], the visible-light photocatalytic degradation efficiency of single Ag NCN nanoparticles for methylene blue approached 100% in 40 min, while Ag NCN microparticles reached only about 70% degradation in 30 min; TiO₂/Ag NCN composite particles achieved 94.1% degradation for methylene blue in 1.5 h [24]. Comparison with literature results demonstrates that the synthesized Ag NCN/ZnNCN composite particles possess high photocatalytic degradation activity for organic dye molecules.

The enhanced photocatalytic activity of Ag NCN/ZnNCN composite particles compared with single ZnNCN and the mechanical mixture of Ag NCN and ZnNCN can be attributed to two factors. First, based on the UV-Vis diffuse reflectance spectra ([Figure 3: see original paper]a), heterostructure formation reduced the band gap energy, enhancing visible-light absorption capability and increasing the generation of photogenerated electrons and holes under the same illumination intensity. Second, the heterostructure may promote separation of photogenerated electrons and holes [24], further improving photocatalytic efficiency.

The photocatalytic degradation kinetics of Rhodamine B by Ag NCN/ZnNCN composite particles followed first-order reaction kinetics, described by the equation:

$$\ln \frac{c_0}{c} = kt$$

where c and c_0 are the equilibrium and initial concentrations of Rhodamine B, respectively, k is the first-order rate constant, and t is the illumination time. Fitting the kinetic data from [Figure 4: see original paper]a yielded the curve shown in [Figure 4: see original paper]b. The fitted curve showed good linearity with a correlation coefficient $R = 0.98386$, indicating that the first-order kinetic equation well describes the photocatalytic degradation process of Rhodamine B by Ag NCN/ZnNCN composite particles, with a rate constant $k = 0.108 \text{ min}^{-1}$.

Conclusions

- (1) Novel flower-like ZnNCN particles and Ag NCN/ZnNCN composite photocatalysts were successfully prepared through a simple ligand exchange reaction. Single ZnNCN particles had a band gap of 4.66 eV, showing strong UV absorption characteristics. The Ag NCN/ZnNCN composite particles formed a heterostructure that reduced the band gap to 2.05 eV, providing good visible-light response.

- (2) Under xenon lamp irradiation, Ag NCN/ZnNCN composite particles exhibited enhanced photocatalytic degradation activity, superior to both single ZnNCN and mechanically mixed Ag NCN+ZnNCN particles. The photocatalytic degradation efficiency for Rhodamine B reached 95.2% within 30 min. The degradation process followed first-order reaction kinetics with a rate constant of 0.108 min^{-1} .

References

- [1] Fujishima A, Honda K. Electrochemical photolysis of water at semiconductor electrode [J]. *Nature*, 1972, 238: 37
- [2] Carey J H, Lawrence J, Tosine H M. Photodechlorination of PCB' s in the presence of titanium dioxide in aqueous suspensions [J]. *Bull. Environ. Contam. Toxicol.*, 1976, 16: 697
- [3] Zhang T T, Qi Y, Liu G, et al. Growth mechanism and photocatalytic activity of NaNbO with controllable morphology [J]. *Acta Metall. Sin.*, 2017, 53: 376 (张婷婷, 祁阳, 刘刚等. 形貌可控 NaNbO 的生长机理和光催化性能 [J]. *金属学报*, 2017, 53: 376)
- [4] Feng X W, Chen H, Jiang F. In-situ ethylenediamine-assisted synthesis of a magnetic iron-based metal-organic framework MIL-53(Fe) for visible light photocatalysis [J]. *J. Colloid Interface Sci.*, 2017, 494: 32
- [5] Pu Y C, Chou H Y, Kuo W S, et al. Interfacial charge carrier dynamics of cuprous oxide-reduced graphene oxide (Cu O-rGO) nanoheterostructures and their related visible-light-driven photocatalysis [J]. *Appl. Catal.*, 2017, 204B: 21
- [6] Martins L M D R S, Alegria E C B A, Hughes D L, et al. Syntheses and properties of hydride-cyanamide and derived hydrogen-cyanamide complexes of molybdenum (IV). Crystal structure of $[\text{MoH}(\text{NCNH}) (\text{Ph PCH CH PPh})][\text{BF}_4]$ [J]. *Dalton Trans.*, 2003, 3743
- [7] Liu X H, Müller P, Kroll P, et al. Synthesis, structure determination, and quantum-chemical characterization of an alternate HgNCN polymorph [J]. *Inorg. Chem.*, 2002, 41: 4259
- [8] Cunha Sónia M P R M, Guedes da Silvaa M Fátima C, Pombeiro A J L. Activation of cyanamide by a molybdenum (0) diphosphinic centre. formation of cyanoimide and its reactivity with electrophiles [J]. *J. Chem. Soc. Dalton Trans.*, 2002, 1791
- [9] Cunha Sónia M P R M, Guedes da Silva M Fátima C, Pombeiro A J L. Mixed dinitrogen—organocyanamide complexes of molybdenum(0) and their protic conversion into hydrazide and amidoazavinylidene derivatives [J]. *Inorg. Chem.*, 2003, 42:
- [10] Deb S K, Yoffe A D. Inorganic cyanamides. physical and optical properties and decomposition [J]. *Trans. Faraday Soc.*, 1959, 55: 106
- [11] Liu X H, Dronskowski R, Kremer R K, et al. Characterization of the magnetic and structural properties of copper carbodiimide, CuNCN, by neutron diffraction and first-principles evaluations of its spin exchange interactions [J]. *J. Phys. Chem.*, 2008, 112C: 11013

- [12] Liu X H, Stork L, Speldrich M, et al. FeNCN and Fe(NCNH) : synthesis, structure, and magnetic properties of a nitrogen-based pseudo-oxide and -hydroxide of divalent iron [J]. Chem. Eur. J. 2009, 15: 1558
- [13] Liu X H, Krott M, Müller P, et al. Synthesis, crystal structure, and properties of MnNCN, the first carbodiimide of a magnetic transition metal [J]. Inorg. Chem., 2005, 44: 3001
- [14] Krott M, Liu X H, Fokwa B P T, et al. Synthesis, crystal-structure determination and magnetic properties of two new transition-metal carbodiimides: CoNCN and NiNCN [J]. Inorg. Chem., 2007, 46: 2204
- [15] Cao R, Tatsumi K. Use of dipotassium cyanamide for the synthesis of cyanoimido (NCN²) complexes of tungsten and cobalt [J]. Chem. Commun., 2002, (18): 2144
- [16] Becker M, Nuss J, Jansen M. Synthese und charakterisierung von Natriumcyanamid [J]. Z. Anorg. Allg. Chem., 2000, 626:
- [17] Becker M, Jansen M. Synthesis of potassium cyanamide, and crystal structure determination by pareto optimisation of the cost functions 'lattice energy' and 'powder intensities' [J]. Solid State Sci., 2000, 2: 711
- [18] Liu X H, Decker A D, Schmitz D, et al. Crystal structure refinement of lead cyanamide and the stiffness of the cyanamide anion [J]. Z. Anorg. Allg. Chem., 2000, 626: 103
- [19] Becker M, Jansen M. Synthese und charakterisierung von quecksilbercyanamid [J]. Z. Anorg. Allg. Chem., 2000, 626: 1639
- [20] Liao W P, Hu C H, Kremer R K, et al. Formation of complex three- and one-dimensional interpenetrating networks within carbodiimide chemistry: NCN²-coordinated rare-earth-metal tetrahedra and condensed alkali-metal iodide octahedra in two novel lithium europium carbodiimide iodides LiEu (NCN)I and LiEu (NCN) I [J]. Inorg. Chem., 2004, 43: 5884
- [21] Becker M, Nuss J, Jansen M. Crystal structure and spectroscopic data of silver cyanamide (in German) [J]. Z. Naturforsch., 2000, 55b: 383
- [22] Zhao W, Liu Y F, Liu J J, et al. Controllable synthesis of silver cyanamide as a new semiconductor photocatalyst under visible-light irradiation [J]. J. Mater. Chem., 2013, 1A: 7942
- [23] Meng H, Li X X, Zhang X, et al. Fabrication of nanocomposites composed of silver cyanamide and titania for improved photocatalytic hydrogen generation [J]. Dalton Trans., 2015, 44: 19948
- [24] Li X, Zhang X, Zhu Z F, et al. Synthesis of TiO /Ag NCN composite catalysts and their photocatalytic activity under visible light irradiation [J]. Chem. J. Chin Univ., 2015, 36: 361 (李霞, 张霞, 朱泽峰等. TiO /Ag NCN 复合光催化剂的制备与可见光催化性能 [J]. 高等学校化学学报, 2015, 36: 361)
- [25] Kaye K M, Grantham W, Hyett G. A facile route to thin films of zinc carbodiimide using aerosol-assisted CVD [J]. Chem. Vap. Deposition, 2015, 21: 281
- [26] Pesika N S, Stebe K J, Searson P C. Determination of the particle size distribution of quantum nanocrystals from absorbance spectra [J]. Adv. Mater., 2003, 15(15): 1289

Note: Figure translations are in progress. See original paper for figures.

Source: ChinaXiv – Machine translation. Verify with original.